Łukasz Rakoczy, Anna Zielińska-Lipiec, Lechosław Tuz, Tomasz Góral

Nd-YAG Laser Beam-Induced Liquation Cracking in Selected Nickel-Based Superalloys

Abstract: MAR-M247 and Rene 77 belong to intermetallic phase $Ni_3(Al, Ti)$ precipitation hardened nickel alloys widely used in the aerospace and power engineering industries. Because of their susceptibility to cracking, the above-named alloys are characterised by limited weldability. In the tests described in this article, the surfaces of the above-named superalloys were affected by a laser beam having identical parameters. Afterwards, the test results concerning the individual susceptibility to Nd-YAG laser beam-induced liquation cracking were compared. The stereoscopic microscopic observations revealed differences indicating the significantly greater crack susceptibility of superalloy MAR-M247. The characteristics of the materials indicated that the above differences were connected with the significantly more complex microstructure resulting from the segregation of alloying elements during crystallisation. The scanning microscopic examination revealed the presence of liquation cracks in the HAZ located along partially melted interdendritic areas.

Keywords: liquation cracking, superalloys, gas turbine

DOI: *10.17729/ebis.2017.1/4*

Introduction

The second half of the 20th century saw the enormous development of nickel-based superalloys resulting from modifications of chemical compositions and manufacturing technologies. Designs of new alloys were triggered by the growing demand for materials operating at very high temperature (primarily in gas turbines) [1-3]. Superalloys MAR-M247 and Rene 77 are widely used in the production of rotor blades and stator blades in aero-engines because of their particularly high strength properties at operating temperature as well as due to their excellent high-temperature corrosion resistance [4]. The aggressive corrosive environment combined with high stresses during the operation of elements in the hot section results (after some time) in damage to parts through creeping, thermo-mechanical fatigue and erosive wear. In most cases, the repair of damaged

mgr inż. Łukasz Rakoczy (MSc Eng.), dr hab inż. Anna Zielińska-Lipiec (PhD (DSc) habilitated Eng.), Professor at AGH; dr inż. Lechosław Tuz (PhD (DSc) Eng.) – AGH University of Science and Technology, Faculty of Metals Engineering and Industrial Computer Science, Department of Physical and Powder Metallurgy; Heat Treatment and Joining Laboratory;
dr inż. Tomasz Góral (PhD (DSc) Eng.) – AGH University of Science and Technology, Faculty of Mechanical Engineering and Robotics, Department of Manufacturing Systems, Unit of Manufacturing Techniques

Table 1. Chemical compositions of the base materials

Alloy/Element	W	Co	Cr	Al	Ta	Hf	Ti	Mo	C	Ni
MAR-M247	10.19	9.92	8.40	5.58	3.12	1.11	0.92	0.64	0.13	rest
Rene 77	0.05	14.55	14.43	4.16	-	-	3.37	3.98	0.06	rest

parts is more convenient (from the economical point of view) than the replacement and the use of new elements (because of high production costs and, usually, long delivery times) [5]. The use of welding methods when joining nickel superalloys both in production and repair is highly desirable as it allows the reduction of the final price of an element. However, the implementation of welding methods in the production and repair of elements made of precipitation hardened alloys is significantly limited because of particularly high crack susceptibility in the HAZ during welding and post-weld heat treatment. Cracks formed during welding processes pose problems both during the design and production of elements characterised by complex geometry. The limited weldability could be attributed to the considerable amount of alloying elements in cast superalloys, and in particular, precipitates of intermetallic phase γ' $Ni_3(Al, Ti)$ [6]. The presence of microcracks, particularly in rotating elements, is undesirable as during operation the above-named cracks begin to develop. Knowing the mechanism related to the formation of liquation cracks and their morphology could provide information enabling the improvement of the reliability of elements and their safe operation.

Test Materials and Methodology

Base materials used in research-related experiments were two nickel-based casting superalloys MAR-M247 and Rene 77. The chemical compositions of the superalloys were identified using a spark emission spectrometer; the results are presented in Table 1. The surface modification involving the use of an ALPHA LASER ALS100 pulsed laser with an Nd-YAG active element was performed on 1.5 mm thick specimens having an area of approximately 2 cm^2 each. The process parameters are presented in Table 2. Changes in the surfaces were observed using a stereoscopic microscope. Hardness measurements concerning the base material were performed using a hardness tester manufactured by Zwick. For the purposes of light and scanning microscopy, metallographic specimens were made. The microstructure of the test superalloys was revealed through etching using Kalling`s reagent and electronically in a 10% solution of Cr_2O_3. The metallographic specimens were performed using a LEICA DM4000 light microscope as well as FEI NOVA NANOSEM 450 and JEOL scanning microscopes provided with an EDS detector (X-ray energy dispersive spectrometer).

Table 2. Parameters of the surface modification process using the laser beam

Voltage [V]	Pulse time [ms]	Frequency [Hz]	Beam diameter [mm]	Energy [J]	Power [W]
244	6.5	3.0	0.8	16.93	50.8

3. Test Results

Base Materials in the As-Delivered State

The microstructures of casting superalloys MAR-M247 and Rene 77 are presented in Figure 1. The microstructure of the casting superalloys was characterised by significant heterogeneity resulting from the segregation of alloying elements during the crystallisation of the alloy (Fig.1a, b). The interdendritic areas contained eutectics γ-γ' (Fig. 1c, d) as well as carbides of various morphology formed through the eutectic reaction with the "Chinese script" type matrix. In alloy Rene 77, the content of eutectic isles γ-γ' and primary carbides was significantly lower. The dendritic cores contained primarily

matrix γ and intermetallic phase γ' $Ni_3(Al, Ti)$ responsible for high mechanical properties of the superalloys. The hardness measurements revealed significant differences of hardness values. MAR-M247 was characterised by hardness over 40HV5 higher than that of Rene 77 (463HV5 and 421HV5 respectively). The high hardness values related to the superalloys were connected with significant precipitation and solid solution hardening. Because of differences of atomic radiuses in relation to Ni, the additions of chromium, cobalt, molybdenum, tungsten or tantalum provided the significant hardening of the plastic matrix (phase γ). Figure 2 presents exemplary carbides (and their morphology) found in alloys MAR-M247 and Rene 77 (along with related EDS spectra).

The addition of strongly carbide-forming elements to alloys is aimed at the precipitation of carbides during the crystallisation of alloys. In addition to intermetallic phase γ', the above-named carbides constitute a factor hardening the matrix. Regardless of morphology, the test superalloys revealed primarily the presence of MC type carbides (Fig. 2a, b). In alloy MAR-M247, the carbides were enriched in Ta and Hf. In turn, as regards alloy Rene 77, the greatest affinity to carbon was that of Ti, therefore the alloy contained carbides rich in the above-named element (Fig. 2c, d). The precipitation of carbides along the boundaries of dendrites aims to improve mechanical properties, i.e. creep resistance at operating temperature.

Surfaces of Superalloys after Laser Beam Modification

A series of single impulses was performed on the specimens. The exemplary view of such surface is presented in Figure 3.

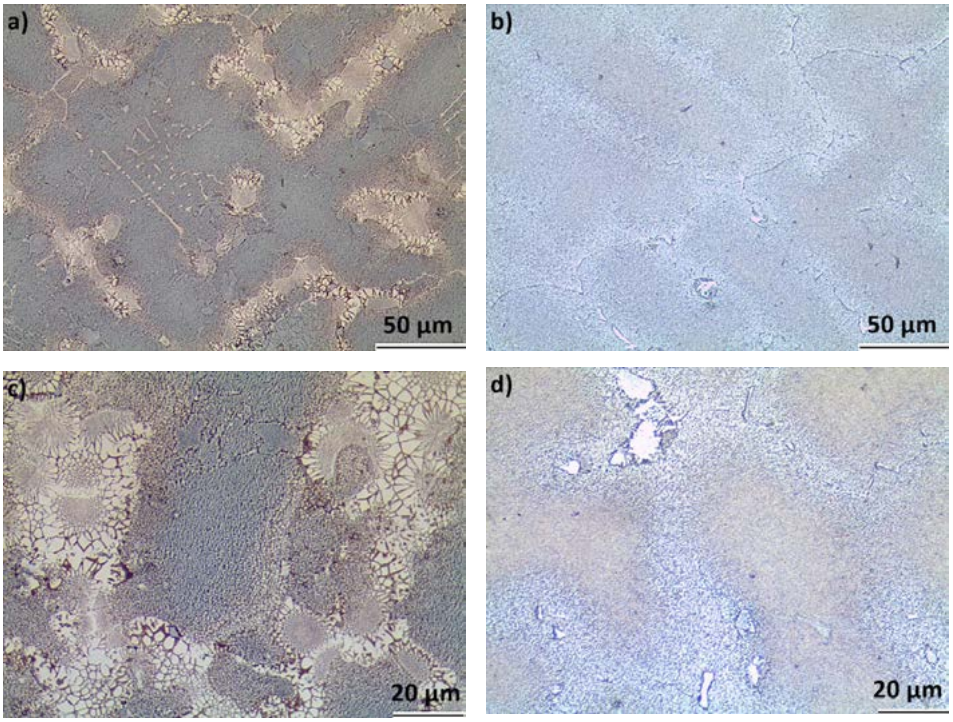

Fig 1. Microstructures of the base materials: a), c) MAR-M247; b), d) Rene 77

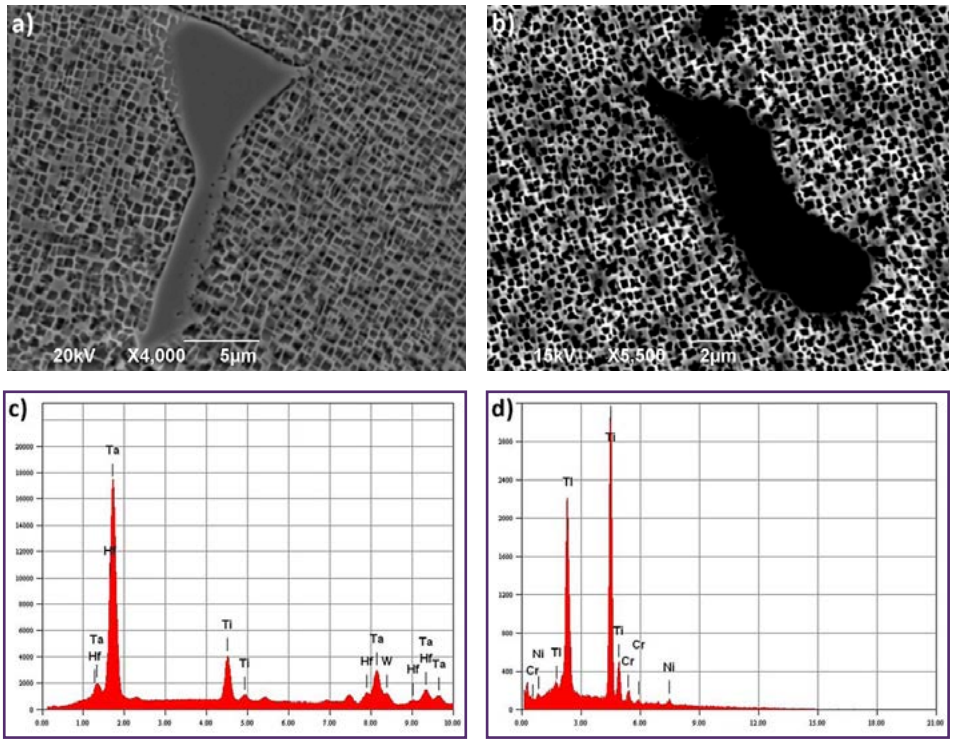

Fig. 2. Microstructure and EDS spectrum of carbides: a), c) MAR-M247; b), d) Rene 77

The short impulse time and related fast heat discharge led to significant changes in the surface. The central areas affected by the laser beam revealed the presence of craters having a depth of approximately 300 μm surrounded by the area having a fairly developed surface. The effect of the laser beam on the surface of superalloy MAR-M247 (Fig. 3a) triggered the formation of several cracks initiated near the crater axis and developing outwards in the direction of the fusion line as well as the formation of smaller cracks of on the periphery. The number of cracks observed in Rene 77 (Fig. 3b) was significantly lower (only a few cracks present at the bottom of the crater). The location of the cracks implied that they were hot cracks formed during the solidification of liquid. The insufficient formability of the alloys resulting from the effect of tensile stresses triggered cracking. The above-named stresses were generated as a result of constrained contraction and the cooling of the molten area.

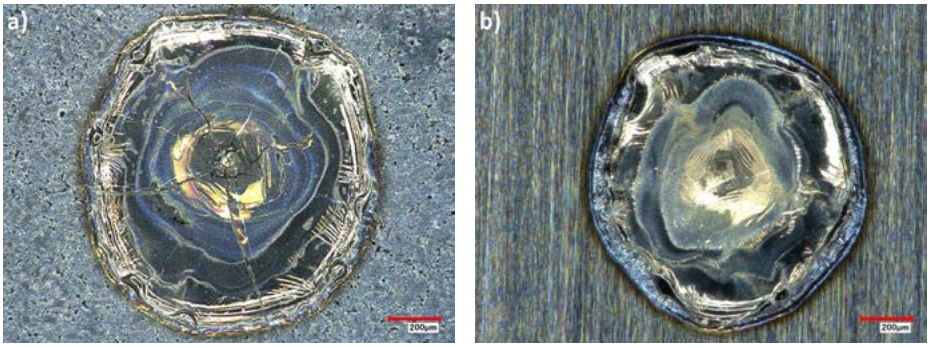

Fig. 3. Surface of the alloys affected by the laser beam: a) MAR-M247; b) Rene 77

Analysis of Cracks in the Heat Affected Zone

The observation of the HAZ susceptibility to crack formation required the performance of tests involving the use of scanning electron microscopes (Fig. 4-7). Alloy MAR-M247 contained a hot crack initiated in the molten area and propagating towards the heat affected zone (Fig. 4a). The liquation crack formation in the HAZ near the fusion line was supported by the hot crack formed previously during the crystallisation of the molten area (demonstrated by its significant width). The crack of purely liquation nature formed as a result of the re-crystallisation through the eutectic transformation with the matrix of the non-equilibrium partially melted phase γ' is presented in Figure 4b. The change in the carbide/matrix interphase surface indicated that the carbides rich in Hf and Ta, characterised by high stability, had been dissolved locally. It cannot be excluded that the partial melting of carbide edges could be ascribed to the change in thermodynamic conditions in the presence of the liquid film. Approximately 60 μm away from the fusion line, the large carbides, underwent brittle cracking (because of the complex state of stresses during cooling) (Fig. 4c).

Superalloy Rene 77 contained numerous liquation cracks located along dendrite boundaries (Fig. 5a). The insufficient amount of liquid

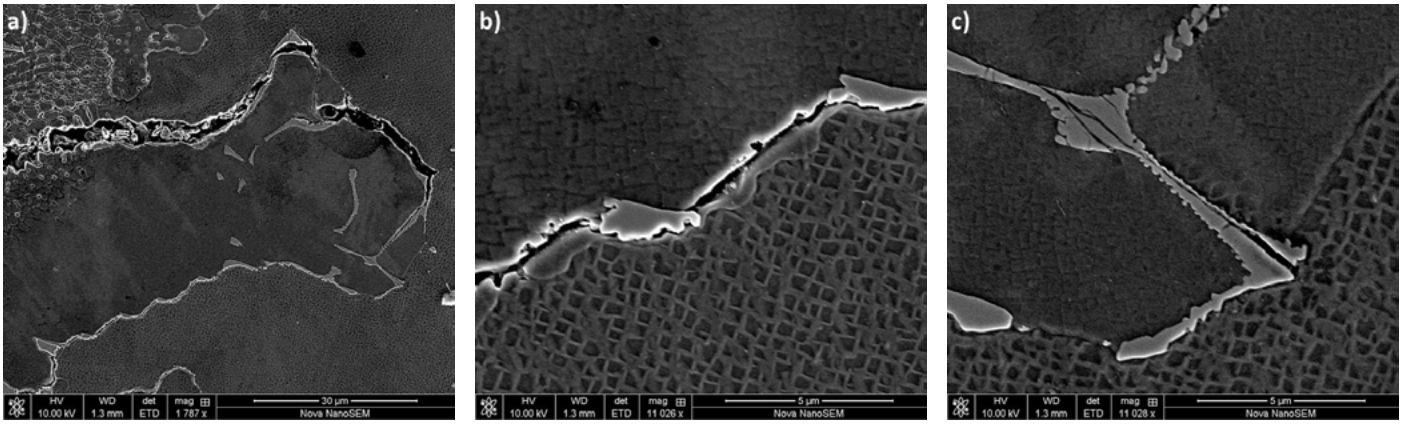

Fig. 4. Liquation cracks in the HAZ in MAR-M247: a) crack location; b) liquation on the boundary of dendrites; c) cracked carbide

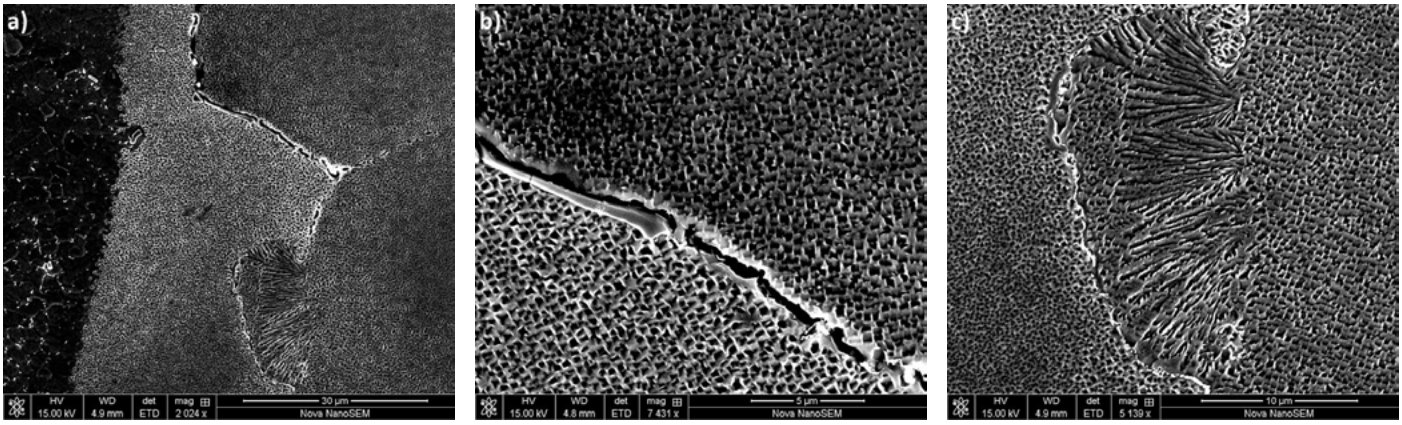

Fig. 5. Liquation cracks in the HAZ in Rene 77: a) crack location; b) liquation on the boundary of dendrites; c) crack propagation towards eutectics γ-γ'

at the final stage of the solidification of the thin interdendritic film triggered cracking (Fig. 5b). The products of eutectic transformation were observed on two opposite edges, except for the carbide area. Fine liquation cracks (Fig. 5c), yet without the clearly visible partial (incipient) melting of the entire area, were observed along the eutectic isle γ-γ' precipitated on the interdendritic boundary.

The morphology of the cracks revealed that the greater crack susceptibility of alloy MAR-M247 was connected with the formation of the greater amount of liquid along dendrite boundaries (during heating). The local partial melting of phase γ' near carbides was also observed outside interdendritic boundaries (Fig. 6).

The primary factor triggering the formation of the liquation cracks was the presence of liquid along dendrite boundaries. The nickel superalloys were characterised by significant segregation, as a result of which microstructural constituents of lower melting point were also present far from the boundaries. The local partial melting (or dissolution) of the intermetallic phase observed in the vicinity of carbides in MAR-M247 and Rene 77 (Fig. 6a, b) indicated that liquation outside the dendrite boundaries did not pose a serious threat. In addition, the molten area contained undissolved, i.e. highly stable, "Chinese script"-like carbides.

The appearance of the crack between dendrites requires both the presence of liquid on the solid-solid boundary and the effect of tensile stresses during cooling. Superalloy Rene 77 contained a boundary along which, at a higher temperature, a relatively thick liquid film was present (Fig. 7). In the created conditions, the interdendritic liquid filled the cracks initiated at a high temperature. The thick liquid film located along the boundaries and the relaxation of stresses by the surrounding material

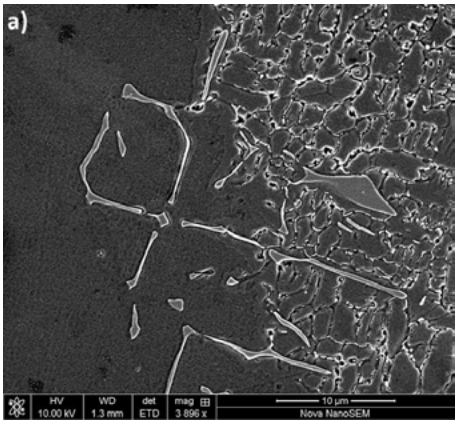

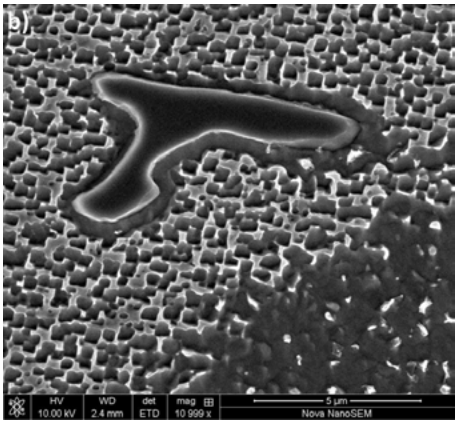

Fig. 6. Local partial melting of phase γ' in the HAZ: a) MAR-M247; b) Rene 77

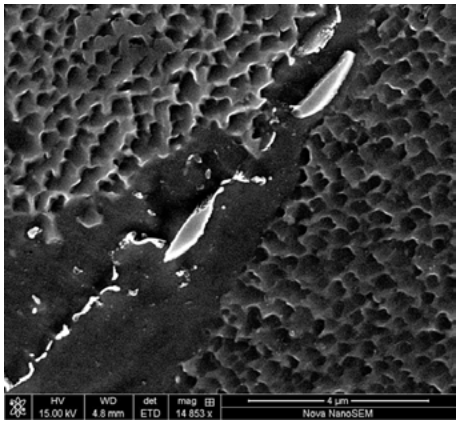

Fig. 7. Partially melted boundary of the dendrites in the HAZ (Rene 77)

precluded the formation of a liquation crack. Similar areas indicating the liquid healing of the microcracks were not observed in superalloy Mar-m247.

Discussion

The presence of liquid on the dendrite boundaries was the primary factor responsible for the liquation cracking in the HAZ. Therefore, it is important to take into consideration factors leading to their formation during welding processes. Cracks were formed as a result of non-equilibrium partial welding below the solidus temperature of the base material referred to in English-language reference publications as constitutional liquation [7, 8]. The precipitation of phase γ' during solidification and the change in thermal expansion were behind stresses affecting the HAZ and being the primary reason for the initiation and propagation of the cracks. As regards crack resistance, liquation in the heat affected zone is considered as highly unfavourable. Because of the formation of the film of the liquid having the non-equilibrium composition, the range of alloy crystallisation temperatures was extended affecting the subsequent reactions during subsequent heating [7, 9]. The use of the laser beam as the heat source (high heating rates) provided favourable conditions as regards the non-equilibrium partial melting. The entire dissolution of phase γ' was preceded by the obtainment of the temperature, where the eutectic transformation between the particle and the surrounding matrix took place. During slow heating in equilibrium conditions, precipitates Ni_3(Al, Ti) became dissolved (through diffusion) in the matrix thus preceding the eutectic transformation of the particles with the matrix. The very high heating rates did not create equilibrium conditions in the alloys [10].

The SEM tests revealed that the analysed alloys represented various sensitivity to liquation cracking. The significantly greater segregation in alloy Mar-m247 favoured the non-equilibrium partial melting. The higher volume fraction of phase γ' resulting from the higher content of Al and the stronger solution hardening of alloy Mar-m247 impeded the relaxation of stresses and, as a result, increased crack susceptibility. The content of the precipitates of phase Ni_3(Al, Ti) related to the increase in crack formation susceptibility in the HAZ could be ascribed to fast re-precipitation during cooling. The crystallisation of the film of the liquid having the non-equilibrium composition extended the range of crystallisation temperatures, thus leading to the extension of the range of high-temperature brittleness and, at the same time, triggering the increase in the level of welding stresses along the partially melted grain boundaries.

According to Borland [11], the film of liquid characterised by appropriate wettability may spread along boundaries filling previously initiated micro-cracks, thus leading to so-called liquid healing. Similar conclusions were formulated by Owczarski in publication concerning cracks in the HAZ of nickel superalloys [12], stating that the cracks were primarily present in the area containing relatively small amounts of liquid in comparison with the more partially melted area near the fusion line. The phenomenon of liquid healing occurs when the liquid film along the boundaries is sufficiently thick to fill the previously initiated hot microcracks [9, 11].

Summary

The study compared the susceptibility to cracking of two intermetallic phase Ni_3(Al, Ti) precipitation hardened nickel alloys, i.e. Mar-m247 and Rene 77. The article compares the mechanism of liquation crack formation in the heat affected zone and presents the morphology of laser beam-triggered cracks. The tests justified the formulation of the following conclusions:

1. The selected superalloys differed significantly in terms of their chemical compositions and primary microstructure, which significantly affected their crack formation susceptibility;

2. The formation of liquid along the boundaries of dendrites was primarily related to the non-equilibrium partial melting of phase γ'. The change in the geometry of carbides along the partially melted boundaries implies that they might have been partially dissolved;
3. The greater amount of liquid formed along the boundaries of dendrites as well as the greater hardening were responsible for the greater susceptibility to liquation crack formation of alloy MAR-M247;
4. The formation of the sufficiently thick liquid film along the partially melted interdendritic areas made it possible to prevent the formation of liquation cracks by the liquid healing of micro-cracks.

References

[1] Reed R.C.: *The Superalloys Fundamentals and Applications*. Cambridge University Press, New York, 2006 https://doi.org/10.1017/CBO9780511541285

[2] Pollock T.M., Tin S.: *Nickel-Based Superalloys for Advanced Turbine Engines: Chemistry, Microstructure, and Properties*. Journal Of Propulsion And Power, 2006, vol. 22, no. 2, pp. 361-374 http://dx.doi.org/10.2514/1.18239

[3] Lacaze A., Hazotte A.: *Directionally Solidified Materials: Nickel-Base Superalloys For Gas Turbines*. Textures and Microstructures, 1990, vol. 13, pp. 1-14 http://dx.doi.org/10.1155/TSM.13.1

[4] Donachie M.J., Donachie S.J.: *Superalloys: a Technical Guide*, 2nd edition, ASM International, OH, USA, 2002 http://dx.doi.org/10.1002/9781118985960.meh108

[5] Carter T.J.: *Common failures in gas turbine blades*. Engineering Failure Analysis, 2005, vol. 12, pp. 237–247 http://dx.doi.org/10.1016/j.engfailanal.2004.07.004

[6] Rush M.T., Colegrove P.A., Zhang Z., Courtot B.: *An investigation into cracking in nickel-base superalloy repair welds*. Advanced Materials Research, 2010, vol. 89-91, pp. 467-472 http://dx.doi.org/10.4028/www.scientific.net/amr.89-91.467

[7] Ojo O.A., Richards N.L., Chaturvedi M.C.: *Contribution of constitutional liquation of gamma prime precipitate to weld HAZ cracking in cast Inconel 738 superalloy*. Scripta Materialia, 2003, vol. 50, pp. 641-646 http://dx.doi.org/10.1016/j.scriptamat.2003.11.025

[8] Montazeri M., Ghaini F.M.: *The liquation cracking behavior of IN738LC superalloy during low power Nd:YAG pulsed laser welding*. Materials Characterization, 2012, vol. 67, pp. 65-73 http://dx.doi.org/10.1016/j.matchar.2012.02.019

[9] Sidhu R.K., Ojo O.A., Chaturvedi M.C.: *Microstructural Analysis of Laser-Beam-Welded Directionally Solidified Inconel 738*. Metallurgical and Materials Transactions A, 2007, vol. 38A, pp. 858-870 http://dx.doi.org/10.1007/s11661-006-9063-8

[10] Ojo O.A., Chaturvedi M.C.: *Liquation Microfissuring in the Weld Heat-Affected Zone of an Overaged Precipitation Hardened Nickel-Base Superalloy*. Metallurgical and Materials Transactions A, 2007, vol. 38A, pp. 356-369 http://dx.doi.org/10.1007/s11661-006-9025-1

[11] Borland J.C.: *Generalized Theory of Super-Solidus Cracking in Welds (and Castings)*. Welding Journal, 1960, vol. 7, pp. 508-512

[12] Owczarski W.A. Duvall D.S., Sullivan C.P.: *Model for Heat-Affected Zone Cracking in Nickel-Base Superalloys*. Welding Journal, 1970, vol. 50, pp. 145-155